A Comparative Study of the Toxic Effects of Monosodium Glutamate and Sunset Yellow on the Structure and Function of the Liver, Kidney, and Testis and the Possible Protective Role of Curcumin in Rats

Original Article

Walaa G. Abdelhamid[1], Mahmoud B. Abdel Wahab[2], Mona E. Moussa[1], Lobna A. Elkhateb[3] and Doaa R. Sadek[3]

[1]Department of Forensic Medicine and Clinical Toxicology, Faculty of Medicine, Ain Shams University, Egypt.

[2]Department of Biochemistry, Poison Control Center, Ain Shams University Hospitals, Cairo, Egypt.

[3]Department of Histology, Faculty of Medicine, Ain Shams University, Cairo, Egypt.

ABSTRACT

Introduction: Monosodium glutamate (MSG) and sunset yellow (SY) are food additives that cause oxidative stress in body tissues. Curcumin has many therapeutic activities including antioxidant, anti-inflammatory, and antitumor properties.

Aim of the Work: This study aimed to compare the toxic effects of monosodium glutamate (MSG) and sunset yellow (SY) on the structure and function of multiple organs and to evaluate the possible protective effect of curcumin.

Material and Methods: Sixty adult male albino rats were divided into six groups. Group I (control). Group II received curcumin. Group III received MSG; group IV received SY. Group V received MSG with curcumin, and group VI received SY with curcumin. All treatments were given daily to rats by oral gavage for 28 days. Blood samples were obtained for biochemical analysis at the end of the experiment. The liver, kidney, and testis were dissected for histological studies.

Results: Monosodium glutamate, and to a lesser extent SY caused a significant increase in body weight and protein carbonyl levels with a significant elevation in liver enzymes, total bilirubin, and lipid profile. Sections in the liver showed fatty degeneration, necrosis, and cellular infiltration. A significant increase in Caspase-3 positive immunoreactivity was also detected. Glomerular atrophy, degenerated tubules, and a significant decrease of BCL-2 positive cells were recorded in the kidney with significantly elevated urea, creatinine, and uric acid levels. In the testis, decreased height of germinal epithelium was confirmed by a significant decrease in PCNA-positive cells, testosterone and LH levels. A significant increase in collagen fibers deposition in the liver, kidney, and testis was noticed. Curcumin ameliorated the deleterious effects of MSG and SY on the structure and function of the examined organs.

Conclusion: Monosodium glutamate had more toxic effects in comparison to SY. Supplementation with curcumin extract could successfully ameliorate their toxic effects through its antioxidant action.

Received: 01 September 2021, **Accepted:** 11 October 2022

Key Words: Curcumin, monosodium glutamate, oxidative stress, protein carbonyl, sunset yellow.

Corresponding Author: Doaa R. Sadek, MD, Department of Histology, Faculty of Medicine, Ain Shams University, Cairo, Egypt, **Tel.**: +20 10 0260 9026, **E-mail:** d.sadek@med.asu.edu.eg

ISSN: 1110-0559, Vol. 46, No. 4

INTRODUCTION

Food additives are substances that are added to foods to enhance flavor, color, texture, nutritional value, and preservation[1]. They are divided into preservatives, taste enhancers, coloring agents, antioxidants, stabilizers, and emulsifiers. It has been noticed that people, especially children, consume food additives in great amounts due to their wide availability, in many food products[2]. The sodium salt of glutamic acid, monosodium L-glutamate (MSG), has 78% glutamic acid and 22% sodium salt and water. It is produced through molasses fermentation from sugar cane or sugar beets, corn sugar, and starch. It is composed of white odorless crystals readily soluble in water[3]. It is the most common food additive used as a flavor enhancer since 1907 with trade names such as Ajinomoto, Chinese salt, and E621[4]. It does not decompose during food processing or cooking; however, it is partially dehydrated and transforms into pyrrolidone-2-carboxylate in hot and acidic environments. It is commonly used in many food products such as chips, noodles, canned soups, flavored flakes, mutton meat, bottled soy or Eastern sauces, and frozen and tested tuna[5]. Monosodium glutamate breaks down in an aqueous solution, releasing free glutamate. Free glutamate attaches to taste receptors in the mouth and activates taste nerves to produce the distinct umami

 DOI: 10.21608/ejh.2022.157628.1756

flavor, which is different from the four basic sensations of sour, salty, sweet, and bitter[6]. Monosodium glutamate is recognized by the WHO and FDA as a safe food ingredient with no established daily upper intake limit[7]. However, Freeman reported that overconsumption of MSG in restaurants resulted in a complex of symptoms termed 'Chinese restaurant syndrome, including dizziness, weakness, numbness, flushing, and headache[8].

Sunset Yellow (SY), identified by E110, is a synthetic yellow azo dye produced from aromatic petroleum hydrocarbons. It is used as a food coloring in foods including dairy products, snack chips, jams, dry drink powders, orange sodas, margarine, ice creams, chocolates, and cake decorations[9]. It is also used in aqueous drug solutions, tablets, capsules, toothpaste, and cosmetics[10]. Even though they are often used, azo dyes are currently regarded as one of the most toxic food additives[11]. However, the available literature regarding their toxicity is still insufficient and quite contradictory with limited work evaluating their cytotoxicity[12]. Currently, SY is forbidden in some countries such as Norway and Finland; however, it is still widely used in many countries including Egypt and the Arab world without any regulations[13].

The usage of natural medicinal plants to lower toxicities has grown in recent years all around the world. Curcumin is an essential component of the plant's rhizomes, Curcuma longa, which belongs to the family (Zingiberaceae)[14]. Curcumin has received a lot of attention lately because it exhibits various therapeutic activities including antioxidant, anti-inflammatory, and antitumor properties[15]. Considering the discrepancies in the literature and the growing safety concern for the use of food additives, the present study aimed to compare the toxic effects induced by MSG and SY on the structure and function of the liver, kidney, and testicles in adult male albino rats and to evaluate the possible protective role of curcumin in ameliorating these abnormalities.

MATERIALS AND METHODS

Chemicals

Monosodium glutamate salt (C5H8NNaO4), purity ≥99%, sunset yellow (C16H12N2O7S2), purity ≥88%, and curcumin powder (C21H20O6), purity ≥65% were purchased from Sigma-Aldrich, USA. MSG, SY, and curcumin powder were then administered after being dissolved in distilled water. All additional compounds were of a high analytical grade.

Experimental animals and ethical approval

Sixty adult male albino rats, weighting about 150±20g were obtained from the Clinical Research Centre of the Faculty of Medicine, Ain Shams University, Egypt. They were kept in typical laboratory settings with a 12-hour light/dark cycle and were given unlimited access to food and tap water. The study was approved by the Faculty of Medicine, Ain shams University Research Ethics Committee [FMASU (R 143) 2022].

Experimental design

The rats were divided randomly into six equal groups following a two-week acclimatization period, as follows:

Group I: Distilled water (D.W.) group (negative control): rats were kept under normal conditions and received distilled water (1mL/100g body weight/day).

Group II: Curcumin (Cur) group: rats received curcumin (150 mg/kg body weight/day)[16].

Group III: MSG group: rats received MSG (600 mg/kg body weight/day)[17].

Group IV: SY group: rats received SY (200 mg/kg body weight/day)[18].

Group V: MSG+Cur group: rats received MSG (as in group III) and curcumin (as in group II).

Group VI: SY+Cur group: rats received SY (as in group IV) and curcumin (as in group II).

All treatments were given orally for 28 days.

Collection of blood samples

Prior to scarification and before the beginning of the trial, all rats were weighted. At the end of the experiment (after the 28-day treatment), rats were sacrificed by cervical dislocation. Glass tubes were used to collect the blood samples, which were then centrifuged for 15 minutes at 4000 rpm after being allowed to coagulate. Serum was then stored at -80ºC for biochemical assay. The following parameters were estimated using Arena Bioscien kits, Egypt.

Hepatic, renal profile, and lipid profiles

Serum ALT and AST were determined by Reitman and Frankel[19] and Murray[20] respectively. Serum γ-glutamyltransferase (GGT) activity was measured by Saw *et al*.[21]. Serum total bilirubin and albumin were performed by Walter and Gerade[22] and Doumas *et al*.[23] respectively. Serum urea concentration was measured by Fawcett and Scott[24]. Serum creatinine and uric acid concentration were estimated by Larsen[25] and Caraway[26], respectively. Measurements of lipid profile (triglycerides, LDL-cholesterol, HDL-cholesterol, and total cholesterol concentrations) were done according to Ibegbulem *et al*.[27].

Determination of testosterone and luteinizing hormone (LH) concentrations

Testosterone hormone level was measured by ALPCO (NH, USA) Elisa kit by Wheeler[28], and LH was determined using Abnova (Taipei, Taiwan) ELISA kit by Kosasa[29].

Determination of protein carbonyl

Serum protein carbonyl (PC) concentration was determined according to the method described by Fields and Dixon[30] where DNPH (Brady's reagent) reacts with aldehyde and ketone groups producing DNP-hydrazone. The distinct UV absorption of DNP-hydrazone was measured using a spectrophotometer at 370 nm. After

derivatization, protein carbonyls were quantified by measuring absorbance at 370 nm and calculating hydrazone concentration using molar extinction coefficient (22000 M 1 cm 1) for dinitro-phenyl hydrazone/mg of protein.

Sample collection for histological studies

The liver, kidney, and testicles were removed from the animals after scarification. They were then immediately preserved in 10% buffered formalin and processed to create paraffin blocks. Hematoxylin and eosin (H and E), Masson's trichrome, and Periodic acid Schiff's reaction (PAS) were used to stain sections cut at a thickness of 5-7µm.

Immunohistochemical studies

A positive-charged slide was used to cut the paraffin sections and were subjected to immune histochemical reaction using an anti-Caspase-3 antibody (Lab Vision, CA, USA.) to detect apoptosis in the liver cells, anti-B-cell lymphoma antibody (BCL-2) (mouse monoclonal antibody- from SIGMA-ALDRICH) to detect anti-apoptotic reaction in the kidney and proliferating cellular nuclear antigen (anti PCNA) (Mouse-anti-human polyclonal antibody, Santa Cruz Biotechnology Dallas Texas USA) to detect the proliferation of the germinal epithelium of the seminiferous tubules. The sections were exposed to a secondary antibody (DAKO, Denmark) for 30 minutes. DAB solution (DAKO, Denmark) was used to develop the reaction for 10 minutes. The slides were then dehydrated, cleaned, and mounted after being counterstained with hematoxylin. The identical procedure was followed while processing negative controls, with the exception of using the primary antibody. Positive reaction: Caspase-3: brown cytoplasmic reaction. BCL-2: brown cytoplasmic reaction. PCNA: brown nuclear reaction.

Morphometric analysis

It was done on a computer in the Histology and Cell Biology Department, Faculty of Medicine, Ain Shams University, using the image analyzer Leica Q win V. 3 program. A Leica DM2500 microscope (Wetzlar, Germany) was linked to the computer. All specimens were subjected to morphometric analysis. Using three separate slides from each animal, measurements were taken (X40). On each slide, the measurement was performed on five randomly chosen non-overlapping fields to measure the mean of the following:

The liver

i. Area percentage of collagen fibers in the liver using Masson's trichrome stain.

ii. Area percentage of liver glycogen in PAS sections.

iii. The number of caspase-3 positive hepatocytes.

The kidney

i. Area percentage of collagen fibers in kidney using Masson's trichrome stain.

ii. The optical density of BCL-2 in the kidney sections.

The testis

i. The thickness of germinal epithelium (µm) in H&E sections of the testis.

ii. Area percentage of collagen fibers in testis using Masson's trichrome stain.

iii. The thickness of the basement membrane in the testis in PAS sections.

iv. The number of PCNA-positive spermatogenic cells.

Statistical analysis

By using version 23 of the Statistical Package for the Social Sciences (SPSS Inc., Chicago, IL, USA), all statistical analyses of biochemical blood tests and histomorphometric studies were carried out. The experiment's findings were presented as mean values and standard deviations. A one-way analysis of variance (ANOVA) was used to assess the significant differences in values, and then a post-doc Tukey multiple comparisons test was used to further analyze the changes between the groups. For all comparisons, *P-value* < 0.05 was considered significant.

RESULTS

Body Weight Gain

Monosodium glutamate- and SY-treated rats showed a significantly higher body weight gain (P<0.05) compared with control rats. While concomitant treatment with curcumin caused a significant reduction in weight gain. No significant change was observed in the body weight of rats concomitantly treated with SY and curcumin compared to controls. (Table 1)

Serum protein carbonyl (PC) levels

A significant elevation in PC levels (P<0.05) was observed in MSG- and SY-treated rats compared to all other groups. This was also noticed in the MSG-treated group compared to the SY-treated group. Monosodium glutamate+cur group showed a significant reduction in PC levels compared to MSG group. However, no significant change in PC levels was seen in SY+cur group compared to control groups. (Table 2)

Hepatic profile

Monosodium glutamate and SY caused a significant increase in ALT activity compared to all other groups. On the other hand, groups concomitantly treated with curcumin showed a non-significant increase in ALT activity compared to control groups. Administration of MSG or SY resulted in a highly significant increase in AST activity as compared to other groups while concomitant administration of curcumin with SY showed a non-significant increase in AST activity compared to controls. A significant increase in GGT activity and total bilirubin

was also noticed in MSG- and SY-treated rats compared to other groups. Co-administration of curcumin with MSG or SY significantly decreased the values of GGT and total bilirubin when compared to those received MSG or SY alone. Albumin levels were significantly decreased in MSG-treated rats compared to other experimental groups. (Table 3)

Renal profile

A significant elevation in serum urea concentration was recorded with the administration of MSG and SY compared to other groups. Concomitant administration of curcumin resulted in a significant decrease in serum urea levels compared to MSG- and SY-treated groups. Monosodium glutamate and SY also caused a significant increase in serum creatinine concentration compared to all other groups. A significant decrease was recorded in serum creatinine levels in rats that received curcumin in addition to MSG or SY compared to rats that received MSG and SY alone. A significant increase in serum uric acid concentration in MSG- and SY-treated rats was also noticed compared to other experimental groups with no significant change in that co-administered curcumin with MSG and SY when compared to control groups (Table 4).

Lipid profile

Administration of MSG and SY caused a significant elevation in serum triglycerides concentrations compared to other groups. Also, LDL concentrations were significantly increased in MSG- and SY-treated rats compared to control groups. Monosodium glutamate data showed a highly significant decrease in HDL concentration compared to other groups. Total cholesterol levels were significantly increased in MSG and SY groups with a significant decrease observed upon administration of curcumin in addition to MSG and SY. (Table 5)

Hormonal profile

The mean serum testosterone and LH levels were significantly lower in MSG- and SY-treated rats compared to control groups, with a significant decrease in the MSG group compared to the SY group. No significant difference was shown in serum testosterone and LH levels of the SY+Cur group when compared to control groups (Table 6).

Histological Results

Examination of the histological sections of the curcumin group (data not shown) showed similar results to that of the negative control group.

Liver sections

The examination of sections stained with hematoxylin and eosin (H&E) of the control group showed normal hepatic architecture. The liver consisted of hepatic lobules. Central veins were seen in the center of the hepatic lobules with cords of hepatocytes radiating from them. These cords were separated by narrow blood sinusoids. The hepatocytes appeared polygonal in shape with central rounded vesicular nuclei and acidophilic cytoplasm. Some hepatocytes were binucleated. Portal tracts were located at the periphery of hepatic lobules and contained branches of the hepatic artery, portal, vein, and bile duct (Figure 1A). In the MSG group, the liver architecture was disturbed with dilated and congested blood sinusoids. Many hepatocytes appeared vacuolated with fatty degeneration; others appeared with pyknotic nuclei. Mononuclear cellular infiltration was frequently seen around most central veins. In addition, many oval cells were noticed in the proliferating bile ductules in the portal areas (Figure 1B). The liver sections of the SY group showed dilated congested, central veins with ruptured endothelial lining. Many hepatocytes appeared vacuolated; others appeared with pyknotic nuclei. The blood sinusoids were frequently seen congested and dilated (Figure 1C). Concomitant administration of curcumin together with MSG- and SY- showed an almost normal appearance of the hepatocytes. However, some hepatocytes showed necrotic changes with some dilated and congested blood sinusoids (Figures 1 D,E). In the MSG+Cur group, mononuclear cellular infiltration was occasionally seen around central veins (Figure 1D).

Masson's trichrome-stained sections

The control group showed few collagen fibers around the central vein and the portal tract and in-between the hepatic cords (Figure 1F). In MSG and SY groups, an increased amount of collagen fibers was noticed around the CV, portal tracts and in between hepatic cords (Figures 1 G,H). While concomitant administration of curcumin with MSG and SY showed few collagen fibers around CV, portal tracts, and in between hepatic cords (Figures 1 I,J) respectively. These results were supported by the histomorphometric data. A significant increase ($P<0.05$) in the mean area percentage of collagen fibers in MSG and SY groups compared to control groups. While a significant decrease was noticed in Monosodium glutamate+Cur and SY+Cur groups compared to MSG and SY alone (Table 7).

Periodic acid Schiff- stained sections (PAS)

In the control group, most hepatocytes showed a strong PAS-positive reaction (Figure 2A). In MSG and SY groups, decreased PAS reaction was noticed in most of the hepatocyte's cytoplasm (Figures 2 B,C). Monosodium glutamate+Cur and SY+Cur groups showed many PAS-positive granules in most of the cytoplasm of the hepatocytes, while few hepatocytes were still seen with weak PAS reaction (Figures 2 D,E) respectively. Also, histomorphometric results showed significant decrease in the mean area percentage of liver glycogen in MSG and SY groups compared to the control group. In MSG+Cur and SY+Cur groups; a significant increase in the mean area percentage of liver glycogen compared to Monosodium glutamate and SY groups was detected (Table 7).

Immunohistochemical stain (Caspase-3)

The examination of Caspase-3 sections of the control liver showed a negative reaction in the cytoplasm of hepatocytes (Figure 2F). However, in the MSG group, most hepatocytes showed a strong positive Caspase-3 reaction (Figure 2G). In the SY group, a moderate number of hepatocytes showed a positive Caspase-3 reaction (Figure 2H). In rats that received curcumin with MSG and SY, mild Caspase-3 reaction was occasionally noticed in hepatocytes (Figures 2 I,J) respectively. Statistical analysis showed a significant increase in the number of hepatocytes with positive Caspase-3 reaction in MSG and SY groups compared to control groups. A significant decrease was noticed in MSG+Cur and SY+Cur groups compared to MSG and SY groups respectively (Table 7).

Kidney sections

The examination of H&E-stained sections of the control kidney showed normal glomeruli with an intact Bowman's capsule and filtration space. Proximal convoluted tubules (PCTs) had rounded small outlines and narrow lumina, and distal convoluted tubules (DCTs) appeared with large oval outlines and wide lumina (Figure 3A). In the MSG group, atrophy of glomeruli was frequently seen. Some renal tubules appeared with vacuolated epithelial lining. Dilatation and congestion of peritubular capillaries (Figure 3B). In the SY group, glomerular atrophy was accompanied with an apparent increase in the number of extra glomerular mesangial cells (Figure 3C). Concomitant administration of curcumin resulted in amelioration of the effects of MSG and SY on the kidney structure. Renal glomeruli and tubules appeared normal. However, some renal glomeruli in the MSG+Cur group were still affected (Figures 3 D,E).

Masson's trichrome-stained sections

In the control group, few scattered collagen fibers were seen around the renal corpuscle and renal tubules (Figure 3F). Increased collagen fiber deposition was noticed intraglomerular and in the interstitium in MSG and SY treated groups (Figures 3 G,H) respectively. While Collagen fibers deposition was decreased with concomitant administration of curcumin in MSG+Cur and SY+Cur groups (Figures 3 I,J) respectively. This was confirmed by significant (P<0.05) increase in the mean area percentage of collagen fibers in MSG and SY groups compared to control groups and a significant decrease in MSG+Cur and SY+Cur groups compared to MSG and SY alone (Table 8).

Periodic acid Schiff- stained sections (PAS)

PAS-stained kidney sections of the control group revealed prominent PAS-positive reaction in basement membranes of renal corpuscles and tubules, brush borders of PCT and mesangial matrix in glomerular corpuscle (Figure 4A). In MSG and SY groups, PAS reaction revealed thickened glomerular and tubular basement membranes and decrease PAS positive mesangial matrix in MSG. In SY treated group, prominent PAS positive mesangial matrix was detected. Decrease in PAS positive brush border of PCT was detected in MSG and SY treated groups (Figures 4 B,C) respectively. In MSG+Cur and SY+Cur groups, the PAS immunoreactivity appeared normal especially in the SY+Cur group (Figures 4 D,E)

Immunohistochemical stain (BCL-2)

The examination of BCL-2 sections of control rats showed positive expression of BCL-2 in some tubular cells (Figure 4F). In MSG and SY groups, mild BCL-2 reaction was noticed in few tubular cells (Figures 4 G,H) respectively. In MSG+Cur and SY+Cur groups, a moderate reaction was noticed in many glomerular and tubular cells (Figure 4 I,J) respectively. Similarly, statistical analysis showed a significant decrease in the mean optical density of BCL-2 in MSG and SY groups compared to control groups. A significant increase in mean optical density of BCL-2 was also noticed in MSG+Cur and SY+Cur groups compared to control, MSG and SY groups (Table 8).

Testis Sections

The examination of sections of the control testis showed closely packed seminiferous tubules with minimal interstitium containing Leydig cells and blood vessels. The germinal epithelium of seminiferous tubules was formed of spermatogonia, primary spermatocytes, and early and late spermatids. Sertoli cells were seen in between the germinal epithelial cells, with many sperms attached to their apical surface. The lumen of the seminiferous tubules was filled with numerous spermatozoa. Germinal epithelium and Sertoli cells were seen resting on regular basement membranes that were surrounded by myoid cells with flattened nuclei. (Figure 5A). However, in MSG and SY-treated rats, there was a noticeable enlargement of the interstitial spaces with congested blood vessels. An apparent decrease in the number of Leydig cells was also noticed. Decrease in thickness of germinal epithelium with large gaps between the cells. Most spermatogenic cells appeared degenerated with dense darkly stained nuclei. (Figures 5 B,C) respectively. Co-administration of curcumin with MSG and SY; resulted in more or less normal Spermatogenic cells lining the seminiferous tubules, whereas empty spaces were occasionally seen between spermatogenic cells (Figures 5 D,E). These microscopic findings were confirmed by a significant decrease (P<0.05) in the thickness of the germinal epithelium in MSG and SY groups compared to the control groups. On the other hand, a significant increase was noticed in MSG+Cur and SY+Cur groups in comparison to MSG and SY groups respectively. No significant difference was noticed between-group the SY+Cur group and the control group (Table 9).

Masson's trichrome-stained sections

Minimal collagen fibers were noticed in the basal lamina of the seminiferous tubules, and in the interstitium of the control group (Figure 5F). In MSG and SY groups, increased deposition of collagen fibers was noticed (Figure 5 G,H) respectively. Collagen fibers deposition was decreased in the groups treated with MSG and SY

concurrently with curcumin (Figures 5 I,J) respectively. These results were supported by a significant (P<0.05) increase in the mean area percentage of collagen fibers in MSG and SY groups compared to control groups and a significant decrease was noticed in MSG+Cur and SY+Cur groups compared to MSG and SY alone (Table 9).

Periodic acid Schiff- stained sections (PAS)

In the control group, a PAS-positive reaction was observed in the thin-walled blood vessels and the thin basal lamina of the germinal epithelium. Acrosomal caps of the spermatid showed PAS-positive reactions at different stages of spermiogenesis up to mature sperms. The caps appeared crescent and faced the Sertoli cells. The glycocalyx of the mature sperms also showed PAS-positive reactions (Figure 6A). In MSG and SY groups, the basal lamina of the germinal epithelium appeared thickened and detached, Absent acrosomal cap and weak PAS reaction in the glycocalyx of mature sperms were also noticed (Figures 6 B,C) respectively. On the contrary, MSG+Cur and SY+Cur groups revealed normal PAS-positive reactions similar to control groups (Figures 6 D,E) respectively. In the same context, statistical analysis showed a significant rise in basement membrane thickness in MSG and SY groups in comparison to the control group while there was a significant drop in groups MSG+Cur and SY+Cur (Table 9).

Immunohistochemical stain (PCNA)

Examination of the control rats showed strong positive PCNA immune reactions in nuclei of spermatogonia and primary spermatocytes (Figure 6F). In rats treated with MSG and SY, few cells showed mild positive PCNA reaction (Figures 6 G,H) respectively. However, sections of the testis treated with curcumin concurrently with MSG and SY showed an increased number of PCNA-positive cells (Figure 6 I,J) respectively. Sertoli cells and Leydig cells exhibited negative PCNA reactions in all examined groups. Similarly, statistical analysis showed a significant decrease in the number of PCNA-positive nuclei in MSG and SY groups compared to control groups. Moreover, a significant increase in the number of PCNA-positive nuclei was noticed in MSG+Cur and SY+Cur groups compared to MSG and SY groups, respectively (Table 9).

Table 1: Effects of MSG and sunset yellow (SY) individually and in combination with curcumin on body weight of all experimental animals

Groups	Initial body weight (g)	Final body weight (g)	Weight gain (g)
Negative control (D.W.)	150.3 ± 12.9	214.6 ± 11.4	64.3 ± 6.9
Cur	150.9 ± 12.5	214.7 ± 9.8	63.8 ± 6.7
MSG	148.1 ± 12.1	247.6 ± 14.1 [ab]	99.5 ± 6.9 [ab]
SY	150.9 ± 14.4	236.9 ± 13.9 [abc]	86 ± 6.1 [abc]
MSG+cur	149.1 ± 12.1	225.9 ± 6.1 [abcd]	76.8 ± 8.4 [abcd]
SY+cur	152.4 ± 12.3	222.6 ± 10.9 [cd]	70.2 ± 6.2 [cde]

Values are represented as mean ± SD. (a) $p < 0.05$ vs. control (D.W.) group; (b) $p < 0.05$ vs. curcumin group; (c) $p < 0.05$ vs. MSG group; (d) $p < 0.05$ vs. SY group; (e) $p< 0.05$ vs. MSG+Cur. D.W: distilled water, MSG: MSG, SY: sunset yellow.

Table 2: Effects of MSG and sunset yellow (SY) individually and in combination with curcumin on serum protein carbonyl (PC) levels of all experimental animals.

Groups	PC (µmol/ mg)
Negative control (D.W.)	5.8 ± 0.6
Cur	5.1 ± 1.1
MSG	20.5 ± 2.4 [ab]
SY	12.3 ± 1.4 [abc]
MSG+cur	8.6 ± 0.8 [abcd]
SY+cur	6.1 ± 0.8 [cde]

Values are represented as mean ± SD. (a) $p < 0.05$ vs. control (D.W.) group; (b) $p < 0.05$ vs. curcumin group; (c) $p < 0.05$ vs. MSG group; (d) $p < 0.05$ vs. SY group; (e) $p < 0.05$ vs. MSG+Cur. D.W: distilled water, MSG: MSG, SY: sunset yellow.

Table 3: Effects of MSG and sunset yellow (SY) individually and in combination with curcumin on the hepatic profile of all experimental animals.

Groups	ALT (IU/L)	AST (IU/L)	GGT(IU/L)	Total bilirubin (mg/ dl)	Albumin (mg/ dl)
Negative control (D.W.)	26.9 ± 5.4	126.6 ± 6.1	7.9 ± 2.2	0.33 ± 0.09	4.45 ± 0.3
Cur	25.3 ± 3.1	125.1 ± 8.8	8.1 ± 2.1	0.35 ± 0.09	4.49 ± 0.2
MSG	49.8 ± 5.9^{ab}	230.5 ± 17.1^{ab}	22.2 ± 3.3^{ab}	0.83 ± 0.15^{ab}	3.29 ± 0.2^{ab}
SY	37.9 ± 1.8^{abc}	166.6 ± 12.3^{abc}	18.3 ± 2.6^{abc}	0.58 ± 0.09^{abc}	4.23 ± 0.1^{c}
MSG+cur	30.3 ± 2.1^{cd}	140.4 ± 4.3^{abcd}	11.3 ± 2.8^{cd}	0.39 ± 0.07^{cd}	4.42 ± 0.2^{c}
SY+cur	27.5 ± 4.6^{cd}	128.2 ± 8.3^{cd}	8.4 ± 2.1^{cd}	0.35 ± 0.07^{cd}	4.33 ± 0.24^{c}

Values are represented as mean ± SD. (a) $p < 0.05$ vs. control (D.W.) group; (b) $p < 0.05$ vs. curcumin group; (c) $p < 0.05$ vs. MSG group; (d) $p < 0.05$ vs. SY group. D.W: distilled water, MSG: MSG, SY: sunset yellow, ALT: Alanine Amino Transferase, AST: Aspartate Amino Transferase, GGT: γ glutamyl transferase.

Table 4: Effects of MSG and sunset yellow (SY) individually and in combination with curcumin on the renal profile of all experimental animals.

Groups	**Urea (mg/ dl)**	**Creatinine (mg/ dl)**	**Uric acid (mg/ dl)**
Negative control (D.W.)	31.5 ± 6.4	0.74 ± 0.08	1.34 ± 0.11
Cur	31.9 ± 4.7	0.73 ± 0.11	1.31 ± 0.15
MSG	78.7 ± 9.5^{ab}	1.62 ± 0.22^{ab}	2.36 ± 0.13^{ab}
SY	50.1 ± 4.9^{abc}	1.24 ± 0.15^{abc}	1.71 ± 0.5^{abc}
MSG+cur	40.1 ± 4.7^{abcd}	0.92 ± 0.11^{cd}	1.32 ± 0.08^{cd}
SY+cur	36.4 ± 3.7^{cd}	0.78 ± 0.12^{cd}	1.33 ± 0.15^{cd}

Values are represented as mean ± SD. (a) $p < 0.05$ vs. control (D.W.) group; (b) $p < 0.05$ vs. curcumin group; (c) $p < 0.05$ vs. MSG group; (d) $p < 0.05$ vs. SY group. MSG+Cur. D.W: distilled water, MSG: MSG, SY: sunset yellow.

Table 5: Effects of MSG and sunset yellow (SY) individually and in combination with curcumin on lipid profile of all experimental animals.

Groups	Triglycerides (mg/dl)	LDL- Cholesterol (mg/dl)	HDL-Cholesterol (mg/dl)	Total Cholesterol (mg/dl)
Negative control (D.W.)	77.8 ± 5.4	31.1 ± 4.6	48.3 ± 5.7	77.4 ± 6.1
Cur	78.2 ± 5.7	31.4 ± 4.9	48.9 ± 7.1	78.5 ± 5.4
(MSG	114.3 ± 5.6^{ab}	82.3 ± 7.9^{ab}	32.2 ± 2.7^{ab}	120.9 ± 9.8^{ab}
SY	105.7 ± 4.2^{abc}	44.9 ± 8.1^{abc}	50.1 ± 3.1^{c}	90.7 ± 7.1^{abc}
MSG+cur	78.9 ± 6.2^{cd}	47.3 ± 5.7^{abc}	48.4 ± 4.8^{c}	84.1 ± 5.4^{c}
SY+cur	76.3 ± 6.1^{cd}	33.2 ± 3.7^{cde}	52.1 ± 3.1^{c}	78.7 ± 4.2^{cd}

Values are represented as mean ± SD. (a) $p < 0.05$ vs. control (D.W.) group; (b) $p < 0.05$ vs. curcumin group; (c) $p < 0.05$ vs. MSG group; (d) $p < 0.05$ vs. SY group; (e) $p < 0.05$ vs. MSG+Cur. D.W: distilled water, MSG: MSG, SY: sunset yellow.

Table 6: Effects of MSG and sunset yellow (SY) individually and in combination with curcumin on serum testosterone and LH of all experimental animals.

Groups	Testosterone (mlU/ml)	LH (mlU/ml)
Negative control (D.W.)	1.89 ± 0.17	32.3 ± 1.46
Cur	1.94± 0.14	32.7 ± 0.79
MSG	0.73 ± 0.12^{ab}	21± 2.1^{ab}
SY	1.2 ± 0.07^{abc}	25.56 ± 0.95^{abc}
MSG+cur	1.6 ± 0.15^{cd}	29.9 ± 0.93^{cd}
SY+cur	1.74 ± 0.14^{cd}	30.45 ± 1.66^{cd}

Values are represented as mean ± SD. (a) $p < 0.05$ vs. control (D.W.) group; (b) $p < 0.05$ vs. curcumin group; (c) $p < 0.05$ vs. MSG group; (d) $p < 0.05$ vs. SY group. D.W: distilled water, MSG: MSG, SY: sunset yellow, LH: Luteinizing hormone.

Table 7: Effects of MSG and sunset yellow (SY) individually and in combination with curcumin on different histological parameters in the liver of all experimental animals.

Groups	Mean area % of collagen fibers	Mean area % of glycogen	Mean number of Caspase-3 positive cells
Negative control (D.W.)	1.43 ± 0.18	34.1± 3.04	2.4±1.1
Cur	1.35 ±0.78	34.73±2.17	2 ± 0.7
MSG	12.89±1.53^{ab}	18.65±1.48^{ab}	50.4±12.78^{ab}
SY	9.83±1.28 ^{abc}	22.68±1.56^{abc}	34.4±3.8^{abc}
MSG+cur	2.7 ±0.67^{cd}	31.88±3.33^{cd}	14.2± 3.2^{abcd}
SY+cur	1.73±0.52^{cd}	33.92±1.32^{cd}	9 ±2.1^{cd}

Values are represented as mean ± SD. (a) $p < 0.05$ vs. control (D.W.) group; (b) $p < 0.05$ vs. curcumin group; (c) $p < 0.05$ vs. MSG group; (d) $p < 0.05$ vs. SY group. D.W: distilled water, MSG: MSG, SY: sunset yellow.

Table 8: Effects of MSG and sunset yellow (SY) individually and in combination with curcumin on different histological parameters in the kidney of all experimental animals.

Groups	Mean area % of collagen fibers	Mean optical density of BCL-2
Negative control (D.W.)	3.06 ±0.21	11.57±0.75
Cur	3±0.16	11.81±1.5
MSG	13.05±1.67 ^{ab}	3.07± 1.2 ^{ab}
SY	10.71±1.37 ^{ab}	4.8±0.51^{abc}
MSG+cur	4.41 ±1.04 ^{abcd}	27.12±3.09 ^{abcd}
SY+cur	3.9 ±0.45^{d}	28.02 ±3.6 ^{abcd}

Values are presented as mean ±SD. (a) $p < 0.05$ vs. control (D.W.) group; (b) $p < 0.05$ vs. curcumin group, (c) $p < 0.05$ vs. MSG group, (d) $p < 0.05$, vs. SY group. D.W: distilled water, MSG: MSG, SY: sunset yellow, Cur: curcumin.

Table 9: Effects of MSG and sunset yellow (SY) individually and in combination with curcumin on different histological parameters in the testis of all experimental animals.

Groups	Mean area % of collagen fibers	Mean thickness of basement membrane (PAS)	Mean number of PCNA-positive germinal cells	Mean thickness of germinal epithelium(µ)
Negative control (D.W.)	3.13±1.22	0.46±0.11	79.01±7.1	95.38±2.32
Cur	3.16±1.08	0.42± 0.08	80.37±6.5	96.06±3.52
MSG	10.8 ±2.7^{ab}	1.5 ±0.16^{ab}	38.00±2.54 ^{ab}	53.20±5.12^{ab}
SY	8.92±1.25 ^{abc}	1.14 ±0.11^{abc}	44±2.34^{abc}	61.7±4.78 ^{abc}
MSG+cur	4.67 ±1.02^{cd}	0.62 ±0.13^{cd}	72.00±8.51^{cd}	86.17±4.74 ^{cd}
SY+cur	4.04 ±0.45^{cd}	0.58 ±0.18^{cd}	74.60±3.91^{cd}	90.9 ±5.59^{cd}

Values are presented as mean ±SD. (a) $p < 0.05$ vs. control (D.W.) group; (b) $p < 0.05$ vs. curcumin group, (c) $p < 0.05$ vs. MSG group, (d) $p < 0.05$, vs. SY group. D.W: distilled water, MSG: MSG, SY: sunset yellow, Cur: curcumin.

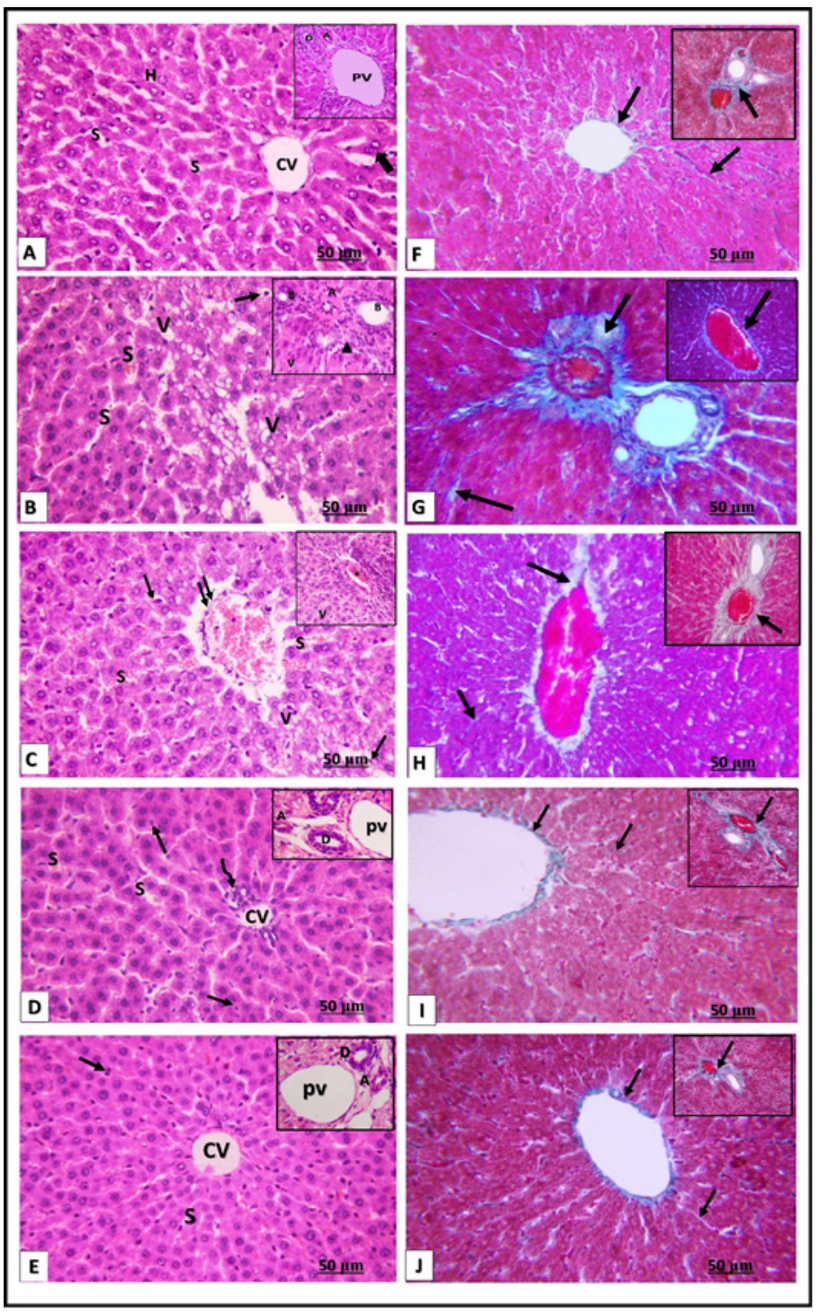

Fig. 1: [A-E] H&E sections of the liver in different groups x400. insets x400, (scale bar: 50 µm). [A] Control group: showing cords of hepatocytes (H) radiating from the central vein. Hepatocytes are separated by the blood sinusoids (S). Hepatocytes appeared polygonal in shape with central rounded vesicular nuclei and acidophilic cytoplasm. Some hepatocytes were binucleated (↑). Inset: showing the portal tract containing branches of the hepatic artery (A), portal vein (PV), and bile duct (D). [B] MSG group: showing loss of normal hepatic architecture with dilated and congested blood sinusoids (S). Some hepatocytes show vacuolations, other cells show pyknotic nuclei (↑). Inset: showing vacuolated hepatocytes with fatty degeneration (V) and oval cells in proliferating bile ductules in the portal area (▲). [C] SY group: Showing dilated congested CV with detached (↑↑) and ruptured (curved arrow) endothelial lining, Vacuolated hepatocytes (V); hepatocytes with pyknotic nuclei (↑) are seen. The blood sinusoids are congested and dilated (S). [inset]: vacuolated (V) hepatocytes and congested portal vein branch (*) are seen. [D] MSG+ curcumin: showing an almost normal structure of hepatocytes. Minimal infiltration of polymorphonuclear leucocytes (curved arrow) is seen around the central vein (CV). Pyknotic nuclei (↑) and dilated congested sinusoids (S) are seen. [E] SY+ curcumin: Some hepatocytes are seen with small darkly stained nuclei (↑) and few blood sinusoids appear dilated and congested (S) (↑). Inset in [D&E]: showing the portal tract containing branches of the hepatic artery (A), portal vein (PV), and bile duct (D). [F-J] Masson`s trichrome-stained sections of the liver of different groups x400, inset x400 (scale bar: 50 µm). [F] Control group showing few collagen fibers (↑) around the central vein and in-between the hepatic cords. Inset: few collagen fibers in the portal tract. [G] MSG group: marked increase in collagen fibers (↑) in the widened portal tract, in-between hepatocytes, and around CV (inset). [H] SY group: increased collagen fibers (↑) is seen around the CV, in between hepatic cords, and in the portal tract (inset). [I&J] MSG+ Curcumin) and (SY+ Curcumin) respectively: few collagen fibers (↑) are seen around CV, in between hepatic cords, and in portal tracts (insets).

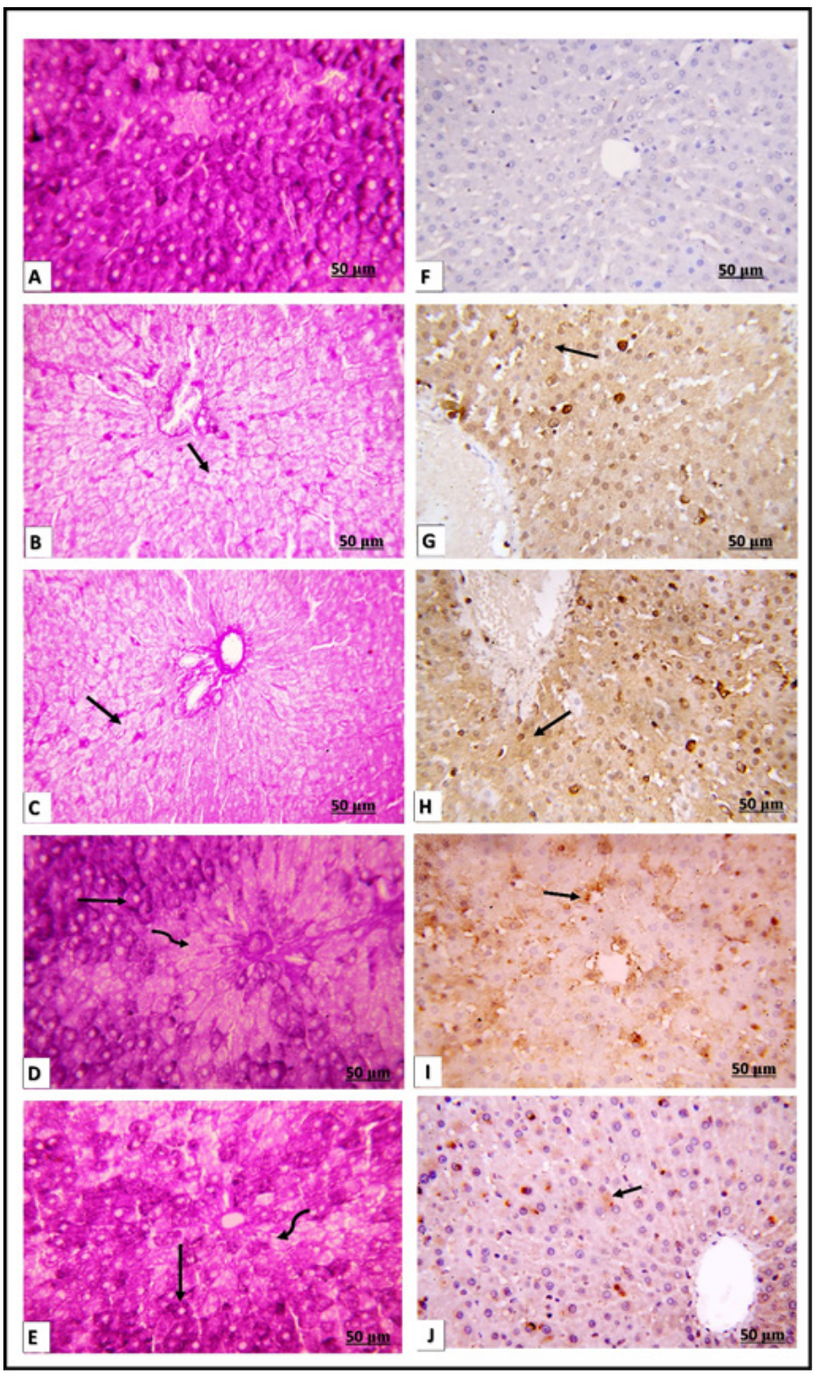

Fig. 2: [A-E] Periodic acid Schiff- stained sections of the liver in different groups x400 (scale bar: 50 µm). [A] Control group: showing strong PAS-positive reaction in most hepatocytes. [B&C] MSG and SY groups respectively: decrease PAS reaction is seen in most hepatocyte cytoplasm (↑). [D&E]: curcumin-treated groups with MSG and SY: show strong PAS-positive reaction (↑) in most hepatocytes. Few hepatocytes are seen with weak reactions (curved arrows). [F-J]: Immunohistochemical stain of Caspase-3 reaction in the liver in different groups x400 (scale bar: 50 µm). [F] control group: showing negative caspase-3 in hepatocytes. [G] MSG group: most hepatocytes have a strong cytoplasmic reaction (↑). [H] SY group: hepatocytes with the cytoplasmic reaction for Caspase-3 (↑) are seen. [I&J] curcumin-treated groups with MSG and SY respectively: mild caspase-3 reaction (↑) is seen.

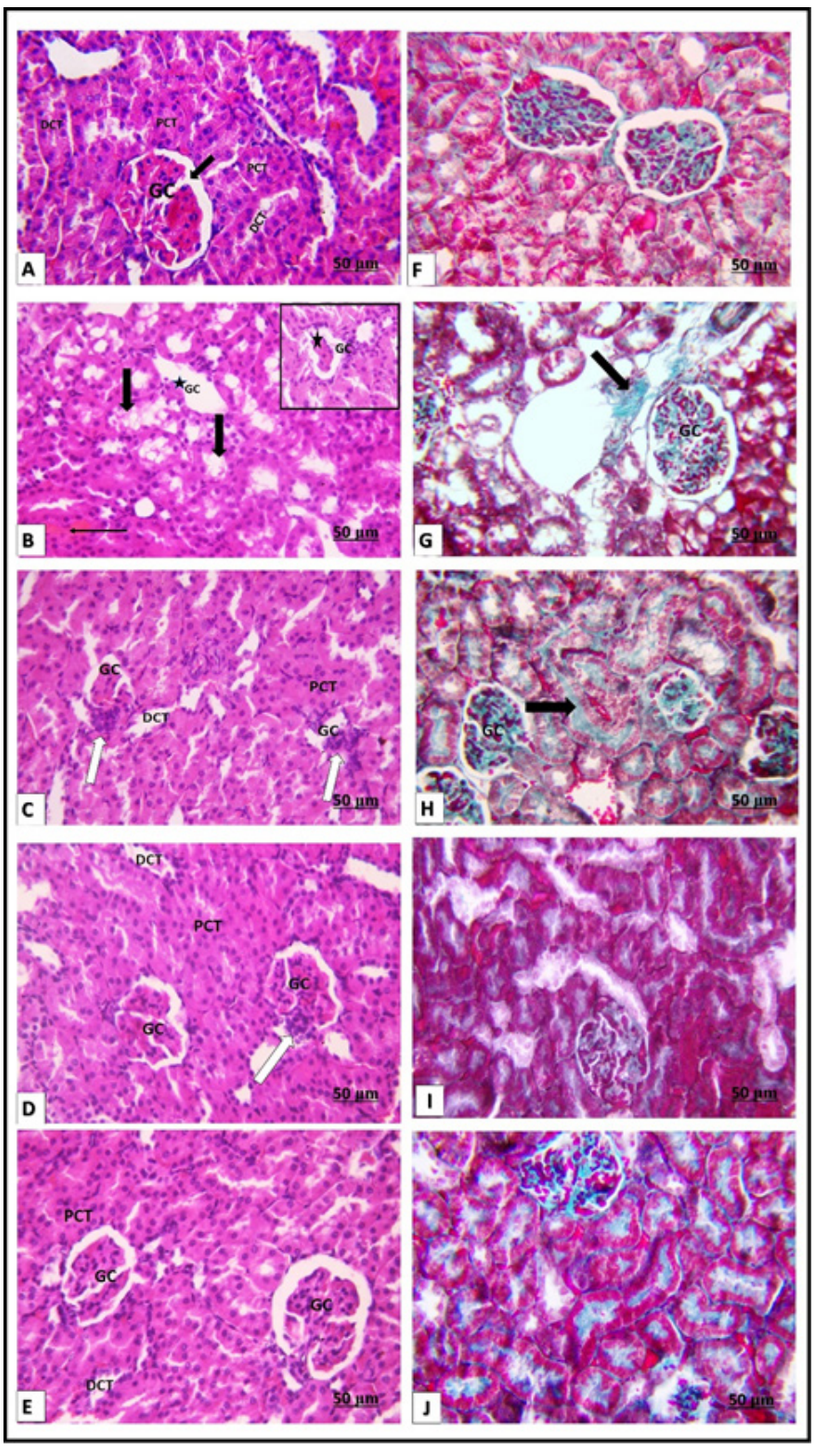

Fig. 3: [A-E] H&E-stained sections in the cortex of the kidney of different groups x400, inset x400 (scale bar: 50 µm). [A] Control group: showing a regular outline of the renal glomerulus (GC). Proximal convoluted tubules (PCT) have rounded small outlines and narrow lumina. Distal convoluted tubules (DCT) appear with a large oval outline and wide lumina. [B] MSG group: showing irregular glomerulus (GC), and shrunken capillaries (*). Most renal tubules appear with vacuolated epithelial lining. A loss of distinction between PCT & DCT (thick arrows) is seen. Sloughed nuclei (↑) are seen inside renal tubules. Inset: shrunken and disturbed (*) glomerulus (GC). [C] SY group: shrunken and hypocellular renal glomerulus (GC) is seen. DCT & PCT are slightly affected. An apparent increase in extra mesangial cells can be seen (white arrow). [D &E] curcumin+ MSG and SY respectively: an almost normal structure of glomerular corpuscle (GC), DCT, and PCT is seen, and extra mesangial cells still appear MSG treated rats with curcumin. [F-J] Masson`s trichrome stained sections of the kidney of different groups x400, (scale bar: 50 µm). [F] Control group: few scattered collagen fibers are seen around renal corpuscles and renal tubules. [G&H]: Increased collagen fibers are seen intraglomerular and in the interstitium after treatment with MSG and SY respectively. [I&J] few collagen fibers are seen after concomitant treatment the rats receive MSG and SY with curcumin respectively.

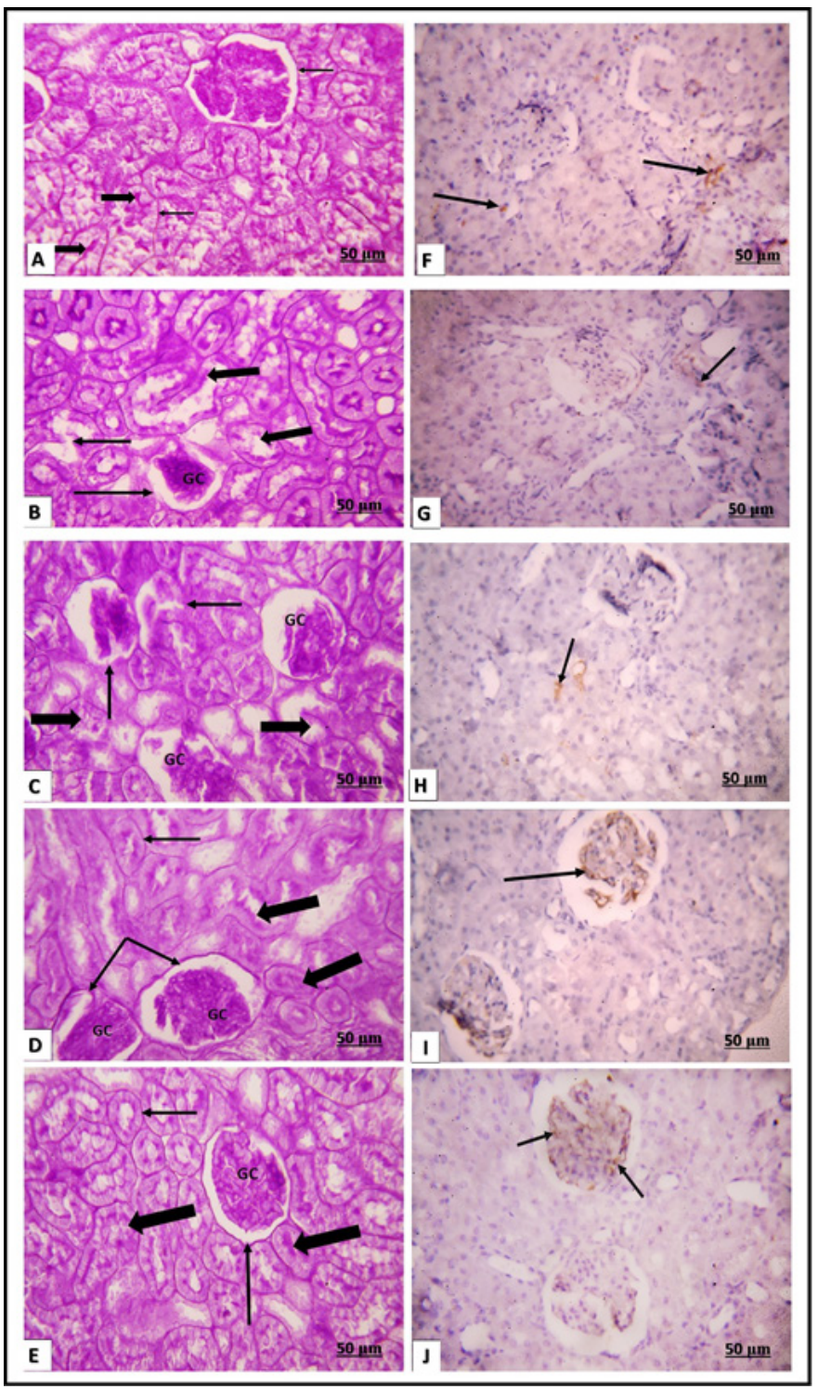

Fig. 4: [A-E] Periodic acid Schiff- stained sections of the kidney in different groups x400 (scale bar: 50 µm). [A] control group: showing prominent PAS-positive mesangium, positive basement membrane in renal corpuscles and tubules (thin arrow). A prominent brush border is also seen in renal tubules (thick arrow). [B&C] MSG and SY groups respectively: showing thick PAS-positive basement membrane (thin arrow). A prominent increase in mesangial tissue is more affected in MSG (GC). A distorted brush border (thick arrow) is seen in some renal tubules. [D&E] curcumin concurrently with MSG and SY respectively: preservation of basement membrane (thin arrow), increase in PAS-positive reaction of the mesangial matrix (GC), and brush border (thick arrow) is seen in renal corpuscles and tubules which is more apparent in the SY+Cur group. [F-J]: Immunohistochemical stain of (BCL2) in the kidney in different groups x400 (scale bar: 50 µm). [F] Control group: showing few cells with positive BCL-2 reaction (↑). [G&H] MSG & SY groups respectively: showing mild cytoplasmic reaction in few tubular cells. [I&J] curcumin concurrently with MSG and SY respectively: increased number and density of BCL-2 positive cells are seen in cells of renal glomeruli.

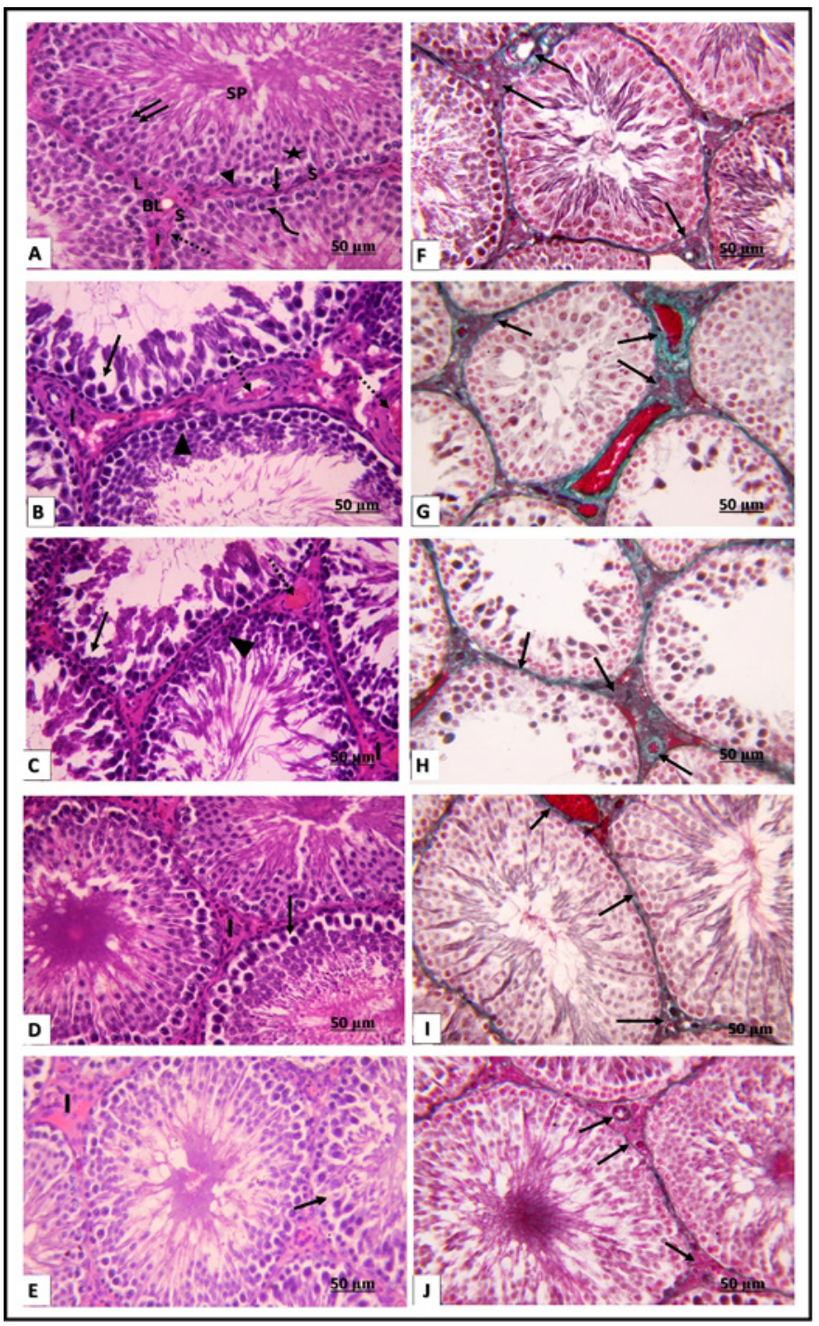

Fig. 5: [A-E] H&E-stained sections of testis in different groups x400, (scale bar: 50 µm), [A] control group: showing closely packed seminiferous tubules and interstitium (I) in-between. Notice the presence of blood vessels (BL) and Leydig cells (L) with their vesicular nuclei. The germinal epithelium is arranged into many rows which are formed of spermatogonia (▲), primary spermatocytes (curved arrow), early (*), and late spermatids (↑↑). In between the germinal epithelium, Sertoli cells (S) are seen with many sperms attached to them. The lumens of the seminiferous tubules are filled with numerous spermatozoa (SP). Germinal epithelium and Sertoli cells rest on a regular basement membrane (dotted arrow) that is surrounded by flattened myoid cells with flattened nuclei (↑). [B]: (MSG group) showing widening of the interstitial spaces (I) between the seminiferous tubules with an apparent decrease in Leydig cells. Homogenous acidophilic exudates and congested thick-walled blood vessels (dotted arrow) are seen. Areas of cell loss and gaps between spermatogenic cells are seen (↑). Spermatogenic cells appear degenerated with darkly stained nuclei (▲). [C] (SY group): showing mild widening of the interstitial spaces (I) between the seminiferous tubules with an apparent decrease in Leydig cells. The nuclei of spermatogenic cells are darkly stained. Areas of cellular loss (↑) are seen between spermatogenic cells. [D&E] curcumin with MSG and SY respectively: the seminiferous tubules are nearly like those of the control group. The interstitial spaces (I) are apparently narrow with few areas of acidophilic exudates and contain Leydig cells. Spermatogenic cells rest on a regular basement membrane. Empty spaces (↑) are seen between spermatogenic cells. [F-J] Masson`s trichrome-stained sections of the testis in different groups x400. (scale bar: 50 µm). [F] Control group: few collagen fibers (↑) are noticed in the basal lamina of the seminiferous tubules, in the wall of blood vessels, and in the interstitium. [G&H] (group IV&V) respectively: an increase in the amount of collagen fibers (↑) is seen in the basal lamina of the seminiferous tubules, in the wall of the blood vessels, and in the interstitium. [I&J] (MSG+ Curcumin) and (SY+ Curcumin) respectively: few collagen fibers (↑) are seen.

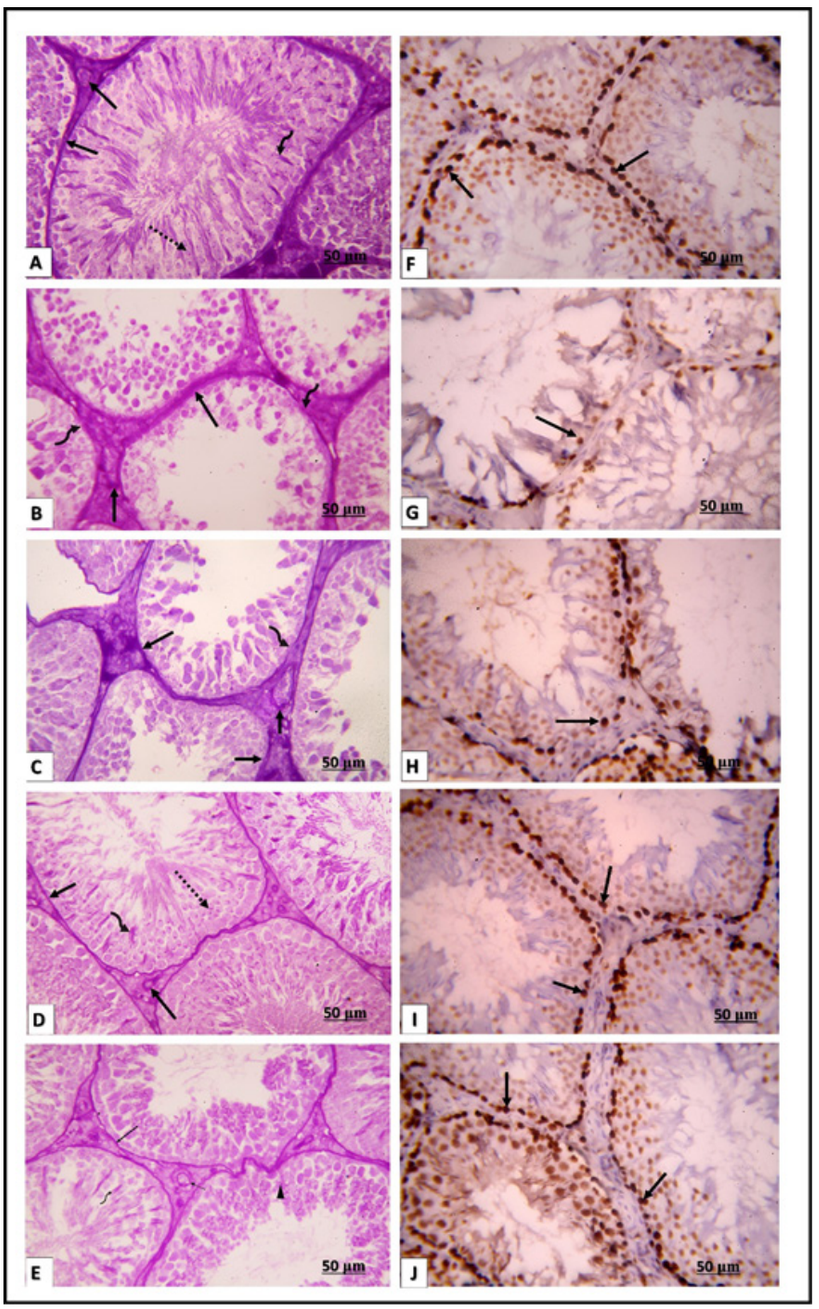

Fig. 6: [A-E] PAS stained sections of the testis in different groups x400 (scale bar: 50 µm). [A]: Control group: showing positive PAS reaction in the basal lamina of blood vessels and basal lamina of the germinal epithelium (↑). Acrosomal caps of the spermatid (dotted arrow) are also stained at different stages of spermiogenesis up to mature sperm. The caps appear crescent and face the Sertoli cells. The glycocalyx of the mature sperms (curved arrow) also appears with a PAS-positive reaction. [B&C] MSG and SY groups respectively: showing thick PAS-positive basal lamina of the germinal epithelium and blood vessels (↑). Areas of the detached basal lamina (curved arrow), absent acrosomal cap, and glycocalyx reactions are also seen. [D&E] curcumin concurrently with MSG and SY respectively show normal PAS reaction. [F-J]: Immunohistochemical stain of (PCNA) in the testis in different groups x400 (scale bar: 50 µm). [F] Control group: positive PCNA reaction is seen in nuclei of spermatogonia (↑). [G&H] (MSG and SY groups) respectively: few spermatogonia are seen with mild PCNA reaction (↑). [I&J] curcumin concurrently with MSG and SY respectively: showing an increase in PCNA immune expression in spermatogenic cells (↑).

DISCUSSION

Despite the current practice all over the world to enhance the flavor and taste of foodstuffs by means of food additives, their increased use could greatly affect human health. The outcomes of our study revealed that rats treated with MSG and SY showed a statistically significant rise in their mean body weight compared with controls. These results agreed with other studies[1,31]. Increased body weight in MSG-treated rats could be attributed to the palatability of food in addition to salt and water retention as a result of increased plasma cortisol levels. Moreover, the hypothalamus does not have an impermeable blood-brain barrier. As a result, free glutamic acid from food could easily reach the hypothalamus, injuring and finally killing its neurons[32]. This leads to impaired leptin and insulin signaling in this region where leptin acts as an appetite-suppressing hormone that controls appetite and body weight[33].

In the present study, a significant increment in protein carbonyl (PC) levels was observed in MSG- and SY-treated rats compared to other groups. Sharma *et al*.[34] found increased PC levels in MSG-treated rats. Previous studies suggested that elevated glutamate levels lead to protein oxidation, oxidative stress, production of reactive oxygen species, and mitochondrial dysfunction. Increased PC levels in SY-treated rats are in line with Qujeq *et al*.[35] where protein oxidation occurred as a direct consequence of an attack by free radicals.

The present work revealed that MSG and SY consumption led to a significant increase in serum lipid profile. On the contrary, HDL-cholesterol showed a significant decrease in the MSG group only compared to other groups. Similar results were recorded by Helal *et al*.[2] and Tawfek *et al*.[18]. Previous studies have proved that ROS could react with thiol moieties producing sulfur oxidant molecules which might attenuate insulin receptor signaling and inhibit cellular uptake of the triglycerides from blood with a subsequent increase in their levels[35]. In addition, MSG was believed to stimulate lipid catabolism via the up-regulation of oxidative genes especially those regulating the bile acid pathway, mainly cholesterol-7-α hydroxylase (CYP7A1)[36]. Furthermore, these changes might be attributed to the mobilization of free fatty acids from adipose tissue to the bloodstream resulting in increased acetyl CoA levels and an increase in cholesterol synthesis or due to lipid peroxidation of cell membranes[37]. The SY showed a less toxic effect on lipid profile which might be due to its minimal direct or indirect action on lipid peroxidation and its potent antioxidant mechanism[18].

In the present study, the histopathological findings in the liver, kidney, and testis were more prominent in MSG than in SY. Similar findings were also observed by El-Borm *et al*.[38]. Monosodium glutamate and SY caused degenerative changes in hepatocytes in the form of fatty degeneration with vacuolations, necrosis, and mononuclear cellular infiltration. Vacuolation of hepatocytes was explained by Cheville[39] who reported that the presence of well-circumscribed vacuoles is characteristic of fatty changes in hepatocytes which may occur due to the collection of the toxic substances to prevent them from interfering with the biological activities of these cells. Other authors suggested that vacuolation of hepatocytes as ballooning degeneration might be a kind of cellular defensive mechanism against toxic substances[40]. Hepatocyte degeneration of the present study was confirmed by a significant increase in caspase 3 positive reaction in Monosodium glutamate and SY groups. Walker and Lupien[41] explained that apoptosis and necrosis are caused by the accumulation of glutamine in hepatocytes resulting in degenerative changes and necrosis. Monosodium glutamate stimulates apoptosis through the formation of reactive oxygen species (ROS) which are associated with oxidative stress[42]. In the current study proliferation of bile ductules lined by vesicular nuclei characteristic of oval cells in rats could be detected. This was in accordance with the results of Schaff and Nagy[43]. They reported that hepatocyte necrosis and degeneration led to a proliferation of the oval cells (stem cells) lining the bile ductules in an attempt to repair the degenerated cells.

The histopathological findings were concomitantly associated with aberrations in biochemical indices. The daily administration of Monosodium glutamate and SY caused a significant increase in serum ALT, AST, GGT, and total bilirubin concentrations when compared to the control rats. These results seemingly agree with Tawfek *et al*.,[18] and AL-Sharkawy *et al*.[44] who attributed this to hepatocellular impairment and liver dysfunction which occurred secondary to increased plasma membrane permeability and cellular necrosis, with subsequent release of intracellular enzymes into the bloodstream. Monosodium glutamate dissociates easily releasing free glutamate followed by the production of ammonium ion (NH4+) that is mostly toxic unless detoxified via the urea cycle in the liver[2]. In addition, free radical production by food additives reacts with fatty acids of the cell membrane leading to mitochondrial dysfunction, destruction of plasma membranes, and finally enzyme leakage[45]. Furthermore, the increased activity of GGT in Monosodium glutamate-treated animals may be due to liver injury resulting from Monosodium glutamate-induced oxidative stress[17]. The drop in albumin levels observed in Monosodium glutamate-treated groups could be attributed to the inhibitory effect of Monosodium glutamate on the biosynthesis of albumin or due to inhibiting the oxidative phosphorylation process. This in turn denoted the liver's inability to perform its functions[46].

In the kidney, Monosodium glutamate and SY affect the structure and function causing atrophy of glomeruli and tubular degenerative changes. The proliferation of extraglomerular mesangial cells could be in the present work. Some authors stated that extraglomerular mesangial cells act as reserve cells that proliferate in response to glomerular atrophy to replace its cells. Other investigators declared that extraglomerular mesangial cells are stem cells

for podocytes[47]. Accumulation of collagen fibers; both inside the glomeruli and in the interstitium of the kidney was detected in the food additive-treated groups of the present study. Some authors declared that Mesangial cells are triggered under pathologic circumstances, resulting in hyperproliferation and an abundance of extracellular matrix (ECM). Also decreased degradation of the mesangial matrix by metalloproteinases occurred. Additionally, mesangial cells secrete many inflammatory cytokines, adhesion molecules, chemokines, and enzymes that all contribute to the development of renal glomerular fibrosis. Interstitial fibrosis was explained by the Epithelial-mesenchymal transition of degenerated tubular cells (EMT) in which the epithelial cells transformed into fibroblasts-like cells features (characterized by the generation of interstitial collagens such as type I and type III)[47].

In the same context, El-Borm *et al*.[38] found degeneration, inflammation, areas of necrosis, vacuolation of renal tubular cells, and glomerular atrophy with Monosodium glutamate. Mahmoud[48] verified that the administration of SY caused destructive changes and necrosis in the liver, kidney, spleen, and brain cell layers of experimental animals. Sharma[7] suggested that oxidative stress is the cause of kidney damage caused by Monosodium glutamate with the formation of ROS which is considered a major cause of nephrotoxic effects leading to cellular and functional damage. Also, El-Borm *et al*.[38] stated that regulated cell death of renal tubules results in membrane-bounded vesicle and crystal nucleation (renal stone). Monosodium glutamate changes renal antioxidant system markers; and reduces activities of superoxide dismutase, catalase, glutathione-S-transferase, and glutathione (GSH) in the kidney. Other authors noticed patchy tubular necrosis and interstitial infiltrations in rats fed with Monosodium glutamate-contaminated food[38]. In the present study, a significant decrease in the mean optical density of BCL2-positive kidney cells was noticed in Monosodium glutamate and SY groups. This might indicate increased cell death because of Monosodium glutamate and SY administration. Khayyat *et al*.[49] reported that BCL2 is an apoptosis regulatory protein that has an anti-apoptotic function, promotes cell cycling, and increases cell resistance to apoptosis.

These structural changes in the kidney affected its function as confirmed by the results of the current kidney function tests where administration of Monosodium glutamate and SY caused a significant increase in serum urea, creatinine, and uric acid concentrations, compared to control groups. Some previous studies reported the same results[2,13,45]. Blood urea is the principal end-product of protein catabolism and is considered a good indicator of kidney functional state; however, elevated serum creatinine concentrations could have a more prognostic significance than other nitrogenous substances in renal diseases[18]. Impaired renal functions might occur following the administration of Monosodium glutamate and SY either because of their metabolites on renal tissues or secondary to oxidative stress. This resulted in interference with creatinine metabolism causing increased synthesis and leading to the impaired functional capacity of tubular excretion[50]. It is suggested that hyperuricemia is accompanied by oxidative stress where xanthine oxidase catalyzes the oxidation of hypoxanthine/xanthine to uric acid with a generation of superoxide radicals[51]. On the contrary, Tawfik and Al-Badr[17] recorded decreased urea concentrations in the Monosodium glutamate group compared to controls attributing this to the impaired urea cycle by food additives with a subsequent decrease in urea production.

Regarding reproductive function, this work demonstrated a significant reduction in serum testosterone levels in the Monosodium glutamate- and SY-treated groups with a significant decrease in the Monosodium glutamate group compared to SY. This agreed with Sakr and Badawy[16] who reported that this might result from a neuronal loss in the hypothalamus with disruption of the hypothalamic-pituitary-testis regulatory axis that controls the production of testosterone by Leydig cells. In addition, oxidative stress inhibits the sensitivity of gonadotrophic cells to gonadotropin-releasing hormone and prevents gonadotropin secretion. Since testosterone and LH are essential for normal testis function and spermatogenesis, therefore, their decrease can adversely affect the reproductive ability of the affected animals[2].

These biochemical analyses were confirmed by the current histological and immunohistochemical results. The rats exposed to Monosodium glutamate and SY showed a widening in the interstitial spaces between seminiferous tubules with homogenous acidophilic exudates and congested blood vessels. Germinal epithelium showed degenerated cells with, vacuolation, exfoliation, and large areas of cell loss which may be signs of testicular toxicity. These results were confirmed by a significant decrease in immunoreactivity for PCNA. Sunset yellow showed a slight decrease in PCNA compared to monosodium glutamate with the presence of PCNA-positive Leydig cells. An increase in the reactivity of PCNA with sunset yellow might be due to a lack of oxidative stress. Oxidative stress results in the withdrawal of cells from the cell cycle.

This was in consideration by Das and Ghosh[52] who noticed that mice exposed to Monosodium glutamate exhibited slight to moderate damage to seminiferous tubules, including vacuolization of spermatogonia and loss of late spermatids. This could also be explained by Storto *et al*.[53] who reported that excessive glutamate dissociated from Monosodium glutamate may hyper-activate the m-Glu receptors present in Sertoli cells resulting in pathological changes in the tubular lumen. Kianifard[54] reported that rats treated with Monosodium glutamate showed atrophy of seminiferous tubules and depletion of germinal epithelium accompanied by derangement of spermatogenic cells. He added that Monosodium glutamate led to the alteration of cellular junction between the spermatogenic cells. A significant decrease in the thickness of the germinal epithelium was noticed in the Monosodium glutamate

group. Alalwani[55] added that the testis is considered a target organ for Monosodium glutamate. The neurotoxins released from Monosodium glutamate could affect the function of the hypothalamus-pituitary-gonadal system.

The congested blood vessels observed in the current study in Monosodium glutamate and SY groups were explained by Balasubramanian *et al*.[56] who attributed them to the inhibition of prostaglandins synthesis since these compounds are known to be involved in the regulation of blood flow.

Increased collagen fibers were noticed in the current study in the liver, kidney, and testis in Monosodium glutamate and SY groups. This was confirmed by the current statistical analysis. Sarhan[57] suggested that the cause of this fibrosis is due to oxidative stress and the formation of ROS which can induce the transformation of fibroblasts to myofibroblasts and increase the deposition of collagen fibers in liver, kidney, and testicular tissues. While Ibrahim *et al*.[58] attributed the cause of fibrosis to the diminished production of glutathione peroxidase.

In the present work, the groups that received daily Monosodium glutamate and SY had a depletion of PAS-positive glycogen content in the liver tissues associated with a significant decrease in glycogen content in hepatocytes, this was in accordance with Dorreia *et al*.[59]. Mustafa *et al*.[60] suggested that Monosodium glutamate stimulates glycogenolysis and gluconeogenesis in the liver leading to a reduction in the glycogen content, hyperglycemia, and a decrease in insulin sensitivity. In the Kidney, the basement membranes appeared thick with a significant increase compared to the control group, and the brush borders of some renal corpuscles were disturbed. There was an apparent increase in the mesangial cells after exposure to SY. Zhao[47] mentioned that intraglomerular mesangial cells, which make up roughly 30–40% of all glomerular cells, are the primary cellular components of the PAS-positive glomerular mesangium. Also, in the testis, there was thickened basal lamina, absent acrosomal cap reaction, and absent glycocalyx reaction in Monosodium glutamate and SY groups with a significant increase in basal membrane thickness compared to the control group. This finding goes in agreement with El-Borm *et al*.[38]. Mahmoud[48] attributed the increased thickness of the basement membranes to the hyperglycemia caused by Monosodium glutamate that enhanced type IV collagen production which is the main component of the basement membranes.

Our study revealed that the addition of curcumin to food additives showed decreased body weight gain compared with the positive treated groups. Teich *et al*.[61] reported similar results, supposing that curcumin administration leads to significant improvement in insulin sensitivity, glucose tolerance, and body fat content with suppression of glucocorticoid action. Curcumin caused a significant decrease in PC levels compared to groups treated with food additives alone. Sakr and Badawy[16] considered curcumin as a powerful antioxidant that inhibited lipid peroxidation by free radical scavenging activity and stimulating endogenous antioxidant enzymes like glutathione peroxidase, glutathione-s-transferase, SOD, and CAT.

Concomitant administration of curcumin with Monosodium glutamate and SY improved the most hazardous effects that occurred in the kidney. A similar finding was also reported by other authors[34]. In our study, curcumin has restored alterations in lipid profile resulting from Monosodium glutamate and SY which is consistent with Ali *et al*.[62] indicating that curcumin prevents increases in serum cholesterol concentrations by inhibiting dietary cholesterol absorption. Curcumin reduced liver enzymes to normal levels and restored albumin levels in the Monosodium glutamate-treated group. A similar observation was also reported by El-Borm[38]. Adewale *et al*.[63] reported that most hepatocytes appeared normal after treatment with curcumin. The cytoprotective effect of curcumin observed in the current study could be explained by its ability to inhibit the oxidative stress induced by food additives by decreasing lipid peroxidation and increasing antioxidant capacity[16]. Curcumin reduces free radical-induced tissue damage, prevents lipid peroxidation, upregulates biosynthesis of various cytoprotective and antioxidant proteins, and inhibits inflammatory cytokines[64].

CONCLUSION

Monosodium glutamate and SY could adversely induce different structural and biochemical changes in the liver, kidney, and testis of adult male albino rats. Monosodium glutamate induced oxidative stress and had more toxic effects in comparison to SY. Supplementation with curcumin extract could successfully ameliorate their toxic effects through its antioxidant action.

FUNDING

There has been no significant financial support for this work that could have influenced its outcome.

CONFLICT OF INTERESTS

There are no conflicts of interest.

REFERENCES

1. El-Helbawy NF, Radwan DA, Salem MF and El-Sawaf ME. Effect of monosodium glutamate on body weight and the histological structure of the zona fasciculata of the adrenal cortex in young male albino rats. Tanta Med J 2017; 45:104–113. DOI: 10.4103/tmj.tmj_11_17
2. Helal E, Barayan A, Abdelaziz MA, EL-Shenawe NS. Adverse Effects of Mono Sodium Glutamate, Sodium Benzoate and Chlorophyllins on some Physiological Parameters in Male Albino Rats. EJHM 2019; 74 (8):1857-1864. DOI: 10.21608/ejhm.2019.28865
3. AL-Mosaibih MA. Effects of Monosodium Glutamate and Acrylamide on the Liver Tissue of Adult Wistar Rats. Life Sci J 2013; 10(2s): 35-42.

4. Leung AY, Foster S. Monosodium glutamate: encyclopedia of common natural ingredients used in food, drugs, and cosmetics. 3rd edition. New York: Nova Science Publishers; 2003. p. 452–454.

5. Eweka AO, Om Iniabohs FAE. Histological studies of the effects of monosodium glutamate on the small intestine of adult Wistar rats. Electron J Biomed 2007; 2:14–18. doi: 10.4297/najms.2010.3146

6. Rolls ET. Functional neuroimaging of umami taste: what makes umami pleasant? Am J Clin Nutr. 2009; 90:804–813. DOI: 10.3945/ajcn.2009.27462R

7. Sharma A. Monosodium glutamate-induced oxidative kidney damage and possible mechanisms: a mini-review. Journal of biomedical science. 2015 Dec; 22(1):1-6. DOI 10.1186/s12929-015-0192-5

8. Freeman M. Reconsidering the effects of monosodium glutamate: a literature review. J Am Acad Nurse Pract 2006; 18:482–486. doi: 10.1111/j.1745-7599.2006.00160.x.

9. Wood R, Foster L, Damant A, Key P. Analytical methods for food additives. CRC Press Boca Raton Boston New York Washington, DC; 2004. p. 274.

10. Helal EG, Abdel-Rahman M. Interaction of sodium nitrate and sunset yellow and its effect on some biochemical parameters in young albino rats. EJHM 2005; 19: 156-167. DOI: 10.21608/EJHM.2005.18118

11. Feng J, Cerniglia CE, Chen H. Toxicological significance of azo dye metabolism by human intestinal microbiota. Frontiers in Bioscience 2012; 4:568-586. doi: 10.2741/400

12. Khayyat LI, Essawy AE, Sorour JM, Soffar A. Sunset Yellow and Allura Red modulate Bcl2 and COX2 expression levels and confer oxidative stress-mediated renal and hepatic toxicity in male rats. Peer J 2018; 1-17. DOI 10.7717/peerj.5689.

13. Abd Elhalem SZ, EL-Atrash AM, Osman AS, Sherif AA, Salim EI. Short-term toxicity of food additive azo dye, sunset yellow (e 110), at low doses, in male sprague-dawley rats. Egypt. J. Exp. Biol. (Zool.) 2016; 12(1):13 – 21.

14. Pari L, Tewas D, Eckel J. Role of curcumin in health and disease. Arch. Physiol. Biochem 2008; 114:127-149. DOI: 10.1080/13813450802033958

15. Ströfer M, Jelkmann W, Depping R. Curcumin decreases survival of Hep3B liver and MCF-7 breast cancer cells: the role of HIF. Strahlenther Onkol 2012; 187:393-400. DOI: 10.1007/s00066-011-2248-0

16. Sakr S, Badawy G. Protective Effect of Curcumin on Monosodium Glutamate-Induced Reproductive Toxicity in Male Albino Rats. Global J. Pharmacol 2013; 7(4): 416-422. DOI: 10.5829/idosi.gjp.2013.7.4.76187

17. Tawfik MS, Al-Badr N. Adverse Effects of Monosodium Glutamate on Liver and Kidney Functions in Adult Rats and Potential Protective Effect of Vitamins C and E. Food and Nutrition Sciences 2012; 3: 651-659. DOI: 10.4236/fns.2012.35089

18. Tawfek N, Amin H, Abdalla A, Fargali S. Adverse Effects of Some Food Additives in Adult Male Albino Rats. Curr Sci Int 2015; 4(4): 525-537.

19. Reitman S, Frankel S. A colorimetric method for the determination of serum glutamic oxalacetic and glutamic pyruvic transaminases. Am J Clin Pathol 1957; 28:56-63. DOI: 10.1093/ajcp/28.1.56

20. Koller A, Kaplan A. The CV Mosby Co St. Louis toronto princeton. Clin Chem. 1984;418:1316-24.

21. Saw M, Stromme JH, London JL, Theodorsen L. IFCC method for g-glutamyl transferase [(g-glutamyl) – peptide:ammino acid g-glutamyl transferase, EC 2.3.2.2]. Clin Chem Acta. 1983; 135:315F- 338F.

22. Walter M, Gerade RW. Bilirubin direct/total. Microchemical Journal 1970; 15: 231-233. doi:10.1016/0026-265X(70)90045-7

23. Doumas BT, Watson WA, Biggs HG. Albumin standard and the measurement of serum albumin with bromocresol green. Clin Chim Acta 1971; 31:87-96. doi: 10.1016/0009-8981(71)90365-2.

24. Fawcett JK, Scott JE. Enzymatic colorimetric method for determination urea in serum, plasma and urine. J. Clin. Path 1960; 13: 156-162. DOI: 10.1136/jcp.13.2.156

25. Larsen K. Creatinine assay by a reaction-kinetic principle. Clin. Chem. Acta 1972; 41: 209-213. DOI: 10.1016/0009-8981(72)90513-x

26. Caraway WT. Determination of uric acid in serum by a carbonate method. American Journal of Clin. Pathol 1955; 2:840-845. DOI: 10.1093/ajcp/25.7_ts.0840

27. Ibegbulem CO, Chikezie PC, Dike EC. Growth rate, haematologic and atherogenic indicators of wistar rats fed with raw and processed cocoa bean-based beverages. J Mol Pathophysiol 2015; 4(2): 77-84. DOI: 10.5455/jmp.20150623092916

28. Wheeler MJ. The determination of bio-available testosterone, Ann. Clin. Biochem. 1995; 32: 345–357. doi/10.1177/000456329503200401

29. Kosasa TS. Measurement of Human Luteinizing Hormone. Journal of Reproductive Medicine 1981; 26:201-206. DOI: 10.1172/JCI105762

30. Fields R, Dixon H. Micro method for determination of reactive carbonyl groups in proteins and peptides, using 2,4-dinitrophenylhydrazine. Biochem J 1971; 121: 587 – 589. DOI: 10.1042/bj1210587

31. Osman AS, Salim EI. Short term toxicity of azo dye, sunset yellow (E110), at low doses, in male sprague-dawley rats. Egypt.j.exp.Biol. (Zool.) 2016; 12(1): 13 – 21.

32. Hawkins RA. The blood brain barrier and glutamate. J Clin Nutr 2009; 90:867–874. DOI: 10.3945/ajcn.2009.27462BB

33. Cekic S, Filipovic M, Pavlovic V, Ciric M, Nesic M, Jovic Z, *et al*. Histopathologic changes at the hypothalamic, adrenal and thymic nucleus arcuatus in rats treated with Monosodium Glutamate. Acta Med Median 2005; 44:35–42.

34. Sharma A, Wongkham C, Prasongwattana V, Boonnate P, Thanan R, Reungjui S, Cha'on U. Proteomic analysis of kidney in rats chronically exposed to monosodium glutamate. PLoS One. 2014 Dec 31;9(12):e116233. doi: 10.1371/journal.pone.0116233

35. Qujeq D, Habibinudeh M, Daylmkatoli H, Rezvani T. Malondialdehyde and carbonyl contents in the erythrocytes of streptozotocin induced diabetic rats. Int. J. Diabetes & Metabolism 2005; 13: 96-98. DOI: 10.1159/000497578

36. Sherif IO, Al-Gayyar MM. Antioxidant,anti-inflammatory and hepatoprotective effects of silymarin on hepatic dysfunction induced by sodium nitrite. Eur. Cytokine Netw 2013; 24(3): 114-121. DOI: 10.1684/ecn.2013.0341

37. Abu Aita NA, Mohammed FF. Effect of marjoram oil on the clinicopathological, cytogenetic and histopathological alterations induced by sodium nitrite toxicity in rats. Glob.Veter 2014; 12(5): 606-616. DOI: 10.5829/idosi.gv.2014.12.05.83186

38. El-Borm HT, Badawy GM, Hassab El-Nabi S, El-Sherif WA, Atallah MN. Toxicity of sunset yellow FCF and tartrazine dyes on DNA and cell cycle of liver and kidneys of the chick embryo: The alleviative effects of curcumin. Egyptian Journal of Zoology 2020; 1(74):43-55. DOI: 10.21608/EJZ.2020.42218.1040

39. Cheville NF. Ultrastructural pathology: the comparative cellular basis of disease. John Wiley & Sons; 2009 Jun 30.

40. Abdel Hameed TF. Light and electron microscopic studies on the effect of orally administered formalin on liver and kidney of guinea pig, Journal of the Egyptian German Society of Zoology C. Histology and Histochemistry 2004; 45 (c): 203-224.

41. Walker R, Lupien JR. The safety evaluation of monosodium glutamate. The Journal of nutrition 2000;130(4):1049S-52S. DOI: 10.1093/jn/130.4.1049S

42. Eweka A and Om'Iniabohs FAE. Histological studies of the effects of monosodium glutamate on the testis of adult wistar rats. The Internet Journal of Urology 2008; 5(2).

43. Schaff Z, Nagy P. Novel factors playing a role in the pathomechanism of diffuse liver diseases: apoptosis and hepatic stem cells. Orvosi hetilap 2004;145(35):1787-93.

44. AL-Sharkawy AN, Gab-Allah MS, El-Mashad AI, Khater DF. Pathological study on the effect of some food additives in male albino rats. BVMJ 2017; 33(2): 75-87. Doi 10.21608/BVMJ.2017.29996

45. Ahmed MH. Effect of some Food Additives Consumption on the Body Weight and Toxicity and the Possible Ameliorative Role of Green Tea Extract. Middle East J. Appl. Sci. 2016; 6(4): 716-730.

46. Abbas MF, Abbas AH. Hepatotoxicity induced by monosodium glutamate (Monosodium glutamate) in rats and the possible hepatoprotective role of n-acetylcysteine. Egypt J. Forensic Sci. Appli. Toxicol, 2016; 16(1):159-178. Doi 10.21608/EJFSAT.2016.39959

47. Zhao JH. Mesangial cells and renal fibrosis. Renal Fibrosis: Mechanisms and Therapies. 2019:165-94. DOI: 10.1007/978-981-13-8871-2_9

48. Mahmoud H. Toxic effects of the synthetic food dye brilliant blue on liver, kidney and testis. The Egyptian Society of Toxicology 2006; 34:77–84.

49. Khayyat LI, Essawy AE, Sorour JM, Soffar A. Sunset Yellow and Allura Red modulate Bcl2 and COX2 expression levels and confer oxidative stress-mediated renal and hepatic toxicity in male rats. PeerJ. 2018 Sep 28;6:e5689. DOI: 10.7717/peerj.5689

50. Masre SF, Nani NN, Razali NA, Yusoff NA, Taib IS. Low Dose Monosodium Glutamate Induced Oxidative Damage and Histopathological Changes on the Renal of Male Rats. Jurnal Sains Kesihatan Malaysia Isu Khas 2019; 33-38. DOI: 10.17576/jskm-2019-17SI-05

51. Paul MV, Abhilash S, Varghese M, Alex MV, Nair RH. Protective effects of α-tocopherol against oxidative stress related to nephrotoxicity by monosodium glutamate in rats. Toxicology Mechanisms and Methods 2012; 22(8): 625-630. DOI: 10.3109/15376516.2012.714008

52. Das R and Ghosh S. Long-term effects of monosodium glutamate on spermatogenesis following neonatal exposure in albino mice. A histological study. Nepal Med. Coll. J. 2010; 12: 149-153.

53. Storto M, Sallese M, Salvatore L, Poulet R, Condorelli DF, Dell'Albani P *et al*. Expression of metabotropic

glutamate receptors in the rat and human testis. J Endocrinol 2001; 170(1):71-8. DOI: 10.1677/joe.0.1700071

54. Kianifard D. Protective Effects of Morus Alba (M. alba) Extract on the Alteration of Testicular Tissue and Spermatogenesis in Adult Rats Treated with Monosodium Glutamate. Medicine Science 2015; 4(1):1947-58.

55. Alalwani AD. Monosodium glutamate induced testicular lesions in rats (histological study). Middle East Fertility Society Journal 2014; 19(4):274-280. doi.org/10.1016/j.mefs.2013.09.003

56. Abd-Elkareem M, Abd El-Rahman MA, Khalil NS, Amer AS. Antioxidant and cytoprotective effects of Nigella sativa L. seeds on the testis of monosodium glutamate challenged rats. Scientific reports. 2021 Jun 29;11(1):13519. DOI: 10.1038/s41598-021-92977-4

57. Sarhan NR. The ameliorating effect of sodium selenite on the histological changes and expression of caspase-3 in the testis of monosodium glutamate-treated rats: Light and electron microscopic study. Journal of microscopy and ultrastructure 2018; 6(2):105. DOI: 10.4103/JMAU.JMAU_2_18

58. Ibrahim M, Khalifa A, Saleh A, Tammam H. Histopathological and Histochemical Assessment of Monosodium Glutamate-Induced Hepatic Toxicity and the Amelioration with Propolis. Ain Shams Journal of Forensic Medicine and Clinical Toxicology 2019; 33(2):24-36. Doi: 10.21608/AJFM.2019.36572

59. Dorreia Az, Mohamed Ad, Hanaa A, Salwa Mo. Effects of monosodium glutamate on the liver of male adult albino rat and the possible protective role of vitamin c (light and electron microscopic study). The Medical Journal of Cairo University. 2018 Dec 1;86(December):3407-18. Doi: 10.21608/MJCU.2018.60313

60. Mustafa SJ, Qader GI, Mahmood SA. Effect of L-Glutamic acid on histology and functions of liver and kidney of rats and protective role of Zingibar Officionale. Diyala Journal of Medicine 2016; 11(2):51-59.

61. Teich T, Pivovarov JA, Porras DP, Dunford EC, Riddell MC. Curcumin limits weight gain, adipose tissue growth, and glucose intolerance following the cessation of exercise and caloric restriction in rats. J Appl Physiol 2017; 123: 1625–1634. DOI: 10.1152/japplphysiol.01115.2016

62. Ali FK, Mohamed A, Hassan AA. Protective Effect of Curcumin on Lipid Profile in Rats Intoxicated by Cyclophosphamide. Egypt. Acad. J. Biolog. Sci. 2021; 13(1):183-188. DOI: 10.21608/eajbsc.2021.184621

63. Adewale OO, Samuel ES, Manubolu M, Pathakoti K. Curcumin protects sodium nitrite-induced hepatotoxicity in Wistar rats. Toxicology reports 2019; 6:1006-11.9. doi: 10.1016/j.toxrep.2019.09.003

64. Abdelhamid FM, Mahgoub HA, Ateya AI. Ameliorative effect of curcumin against lead acetate–induced hemato-biochemical alterations, hepatotoxicity, and testicular oxidative damage in rats. Environ Sci Pollut Res 2020; 27(10):10950-10965. doi: 10.1007/s11356-020-07718-3. doi: 10.1007/s11356-020-07718-3.

الملخص العربى

دراسة مقارنة للتأثيرات السامة للجلوتامات أحادي الصوديوم وأصفرالغروب على بنية ووظيفة الكبد والكلى والخصيه والدور الوقائي المحتمل للكركمين في الجرذان

ولاء جمعه عبد الحميد[١]، محمود بدر عبد الوهاب[٢]، منى القطب موسى[١]، لبنى عبدالرزاق الخطيب[٣]، دعاء رمضان صادق[٣]

[١]قسم الطب الشرعى والسموم الاكلينكيه، كليه الطب، جامعه عين شمس

[٢]قسم الكيمياء الحيوية، مركز مكافحة السموم، مستشفيات جامعة عين شمس

[٣]قسم الهستولوجيا، كليه الطب، جامعه عين شمس

المقدمة: الإضافات الغذائية هي منتجات تضاف إلى الطعام لحفظه ولتحسين النكهة واللون، ويعتبر الجلوتامات أحادي الصوديوم وأصفرالغروب من الإضافات الغذائية التي تسبب الإجهاد التأكسدي في أنسجة الجسم. ويحتوي الكركمين على العديد من الخصائص العلاجية بما في ذلك الخصائص المضادة للأكسدة والمضادة للالتهابات والمضادة للأورام.
هدف الدراسة: هدفت هذه الدراسة إلى مقارنة الأثار السُمية التي يسببها الجلوتامات أحادي الصوديوم وأصفر الغروب على أنسجة الكبد ، والكلية ، والخصية ، وتقييم التأثير الوقائي المحتمل للكركمين في تخفيف سميتها.
طريقة البحث: تم تقسيم ستين من ذكور الجرذان البالغة إلى ست مجموعات. المجموعة الأولى (مجموعة الضبط)، بينما تلقت المجموعة الثانية الكركمين كما تم إعطاء المجموعة الثالثة جلوتامات أحادي الصوديوم والمجموعة الرابعة أصفر الغروب، في حين تناولت المجموعة الخامسة جلوتامات أحادي الصوديوم مع الكركمين ، وتلقت المجموعة السادسة أصفر الغروب مع الكركمين. تم إعطاء جميع العلاجات للجرذان يومياً عن طريق الحقن الفموي لمدة ٢٨ يوماً. في نهاية التجربة، تم الحصول على عينات الدم لإجراء التحليل الكيميائي الحيوي وكذلك تم تشريح الكبد والكلى والخصية للدراسات النسيجية.
النتائج: يُسبب الجلوتامات أحادي الصوديوم ، وبدرجة أقل أصفر الغروب ، زيادة كبيرة في وزن الجسم النهائي ومستويات كاربونيل البروتين. تم الكشف عن التغيرات التنكسية والتسلل الخلوي في أقسام الكبد مؤكدة بزيادة معنوية في إنزيمات ناقل أمين الأسبارتات، وناقل أمين الألانين ، وناقل الجاما جلوتاميل ، وكذلك البيليروبين الكلي بالدم. بالإضافة إلى ذلك ، تلاحظ ارتفاع في مستويات الدهون الثلاثية في الدم ، وكوليسترول البروتينات الدهنية منخفضة الكثافة ، والكوليسترول الكلي. أظهرت المقاطع في الكبد تنكسًا دهنيًا ونخرًا وتسللًا خلويًا مُنعكساً من خلال زيادة خلايا الكبد الإيجابية لكاسبيز-٣. وفي الكلى ، تسببت الإضافات الغذائية في ضمور الكبيبات مع تآكل الأنابيب المصحوبة بزيادة كبيرة في اليوريا ، والكرياتينين ، وحمض البوليك ، وانخفاض في الجسم المضاد لسرطان الغدد الليمفاوية للخلايا البائية. أما في الخصية ، فقد أظهرت الظهارة الجرثومية مناطق كبيرة من فقدان الخلايا مع وجود فجوات كبيرة بين الخلايا أكدها انخفاض كبير في مستويات هرمون التستوستيرون وهرمون مُلْتَوَن وانخفاض في تفاعل مُسْتَضد النواة الخلوية المتكاثِر الإيجابي في الخلايا المولدة للحيوانات المنوية. كما لوحظ زيادة ذات دلالة إحصائية في ترسب ألياف الكولاجين في الكبد والكلى والخصية. قد خفف الكركمين من التأثيرات الضارة للجلوتامات أحادي الصوديوم وأصفر الغروب على بنية ووظيفة الكبد والكلى والخصية.
الخلاصة: يمكن أن يتسبب الجلوتامات أحادي الصوديوم وأصفر الغروب في إحداث تغييرات هيكلية وكيميائية حيوية مختلفة في الكبد والكلى والخصية عند ذكور الجرذان البيضاء البالغة. تسبب الجلوتامات أحادي الصوديوم في الإجهاد التأكسدي وكان له تأثيرات سامة أكثر مقارنةً بأصفر الغروب ويمكن لمستخلص الكركمين أن يخفف بنجاح من آثارها السامة من خلال عمله كمضاد للأكسدة.